Atmos. Chem. Phys. Discuss., 14, 24183–24220, 2014
www.atmos-chem-phys-discuss.net/14/24183/2014/
doi:10.5194/acpd-14-24183-2014

Atmospheric Chemistry and Physics Discussions

Methane as a diagnostic tracer of changes in the net circulation of the middle atmosphere

E. E. Remsberg

Science Directorate, NASA Langley Research Center, 21 Langley Blvd., Mail Stop 401B, Hampton, VA 23681, USA

Received: 21 August 2014 – Accepted: 9 September 2014 – Published: 18 September 2014

Correspondence to: E. E. Remsberg (ellis.e.remsberg@nasa.gov)

Published by Copernicus Publications on behalf of the European Geosciences Union.

Abstract

This study makes use of time series of methane (CH_4) data from the Halogen Occultation Experiment (HALOE) to determine whether there were any statistically significant changes of the net circulation within the stratosphere and lower mesosphere during 1992–2005. HALOE CH_4 profiles in terms of mixing ratio vs. pressure-altitude are binned into subtropical and extratropical latitude zones of the southern and of the Northern Hemisphere, and their separate time series are then analyzed using multiple linear regression (MLR) techniques. A positive trend in the subtropics and a negative trend in the extratropics is interpreted as indicating an acceleration of the net circulation. A significant acceleration is found in the Northern Hemisphere from 20 hPa to 7 hPa, a likely indication of changes from the effects of wave activity during those years. No similar acceleration is found in the Southern Hemisphere. The trends from HALOE H_2O are analyzed and compared with those from CH_4 for consistency because H_2O is a primary product in the upper stratosphere of the chemical conversion of CH_4. The CH_4 and H_2O trends have a ratio of nearly 2 : 1, and they are anti-correlated most clearly near the stratopause in the southern extratropics. Seasonal anomalies are found in the HALOE CH_4 time series of the lower mesosphere, and they are ascribed to wave-driven, secondary residual circulation cells associated with the descent of the SAO westerlies. The time series residuals for CH_4 of the lower mesosphere also exhibit aperiodic structure, and it is anti-correlated with that of the tracer-like species HCl. Such structure indicates the effects of variations in the wave forcing. It is concluded that multi-year, global-scale distributions of CH_4 are very useful for diagnosing large-scale changes of the net transport within the middle atmosphere.

1 Background

The Brewer/Dobson circulation (BDC) is primarily a seasonal net circulation in the stratosphere, having an upward component at low latitudes and a return, downward

ACPD
14, 24183–24220, 2014

component at the extratropical latitudes of the northern and the Southern Hemispheres (e.g., Butchart, 2014; Plumb, 2007). The BDC has also been referred to as the transformed Eulerian mean (TEM) and residual circulations, and they are useful for viewing the net atmospheric response to the seasonal changes in the diabatic heating (Dunkerton, 1978). The dissipation of Rossby and gravity wave forcings tend to accelerate the net circulation of the winter hemisphere (e.g., Solomon et al., 1986; Plumb, 2007; Shepherd, 2007; Okamoto et al., 2011). In addition, any two-way, meridional exchange or mixing of the air contributes to the primary BDC (Garny et al., 2014). Thus, it is likely that there should be some asymmetry between the seasonal net circulations of the Northern and Southern Hemispheres because the winter wave forcing and mixing processes are more pronounced in the Northern Hemisphere (Shepherd, 2007).

A schematic of the net circulation and its relation to the distribution of ozone in the stratosphere is shown in Fig. 1 for March, where the solid black curves represent the sense of the net circulation and the vertical orange arrow represents the approximate region for the propagation of waves from the upper troposphere and into the middle atmosphere (see Shaw and Shepherd, 2008). Figure 1 indicates that the net circulation during winter and into spring leads to an accumulation of ozone in the extratropics of the Northern Hemisphere by March. Tracer-like molecules, such N_2O and CH_4, exhibit distributions that are well correlated and vary seasonally in response to changes in the net circulation (Plumb and Ko, 1992).

Figure 2 is an example of the zonally-averaged distribution of CH_4 for January from a NASA/Goddard chemistry and transport model simulation (Fleming et al., 1999). The white arrows show the stratospheric Brewer–Dobson circulation, which is strongest in the winter hemisphere (longer arrows), and weak in the summer stratosphere. Tracer fields such as CH_4 reflect the circulation, i.e., bulging upward in the tropics and downward at high latitudes (more so in the winter hemisphere). Figure 2 shows that the January net circulation is in the correct sense to bring about the accumulation of ozone in the lower stratosphere by March, as shown in Fig. 1. In addition, Manney et al. (1994) emphasize that the character of the observed winter hemisphere transport and descent

ACPD
14, 24183–24220, 2014

differs for the upper vs. the lower stratosphere and depends on whether the polar vortex is undisturbed and centered on the Pole or disturbed by Rossby-wave activity.

A current issue is whether the observed, seasonal net circulation is changing in the presence of the steady increases in the so-called "greenhouse gases", like CO_2 (e.g., Butchart, 2014). Early on, Rind et al. (1990) conducted a series of simulation studies of those effects, and their results indicated that there will be an acceleration of the net circulation, particularly in the Northern Hemisphere. Lin and Fu (2013) analyzed more recent results from a collection of chemistry/climate models (CCM), and they found that the diabatic effects from changes in the ozone and CO_2 are likely driving observed changes in the meridional temperature gradients and of the BDC of the lower stratosphere. Based on the results of the CCM studies, they decomposed the BDC into a transition (100–70 hPa) branch, a shallow (70–30 hPa) branch, and a deep (30 hPa and higher) branch. Further, the CCM studies predict an acceleration of the BDC that will affect the rate of recovery for the ozone layer in the lower stratosphere.

Observational evidence of a long-term acceleration of the several branches of the BDC is not so clear from time series of temperature or chemical tracers (Butchart, 2014). Garcia et al. (2011) recommend using observed tracers that are well sampled and have a near-linear growth rate. Hydrogen fluoride (HF) is a stratospheric end product of the photochemical conversion from chlorofluorocarbon molecules but has been increasing non-linearly, so it is not a good candidate for such studies. H_2O has shown long-term increases of about 0.6 % yr^{-1} (Scherer et al., 2008), but H_2O entering the stratosphere from below is subject to seasonal and occasional episodic changes of the temperature at the tropical tropopause. CH_4 exhibits a small, monotonic, and nearly linear, annually-averaged trend in the troposphere, and it is unaffected during upward transport through the tropical tropopause, unlike H_2O.

The modeled CH_4 distribution in Fig. 2 is very similar to observed wintertime distributions of CH_4 from satellite datasets. CH_4 decreases with pressure-altitude and with latitude because CH_4 is oxidized in a multi-step process to H_2O in the middle and upper stratosphere (e.g., Brasseur and Solomon, 2005). In an early study using CH_4

ACPD
14, 24183–24220, 2014

data from the Stratospheric and Mesospheric Sounder (SAMS) on Nimbus 7, Stanford and Ziemke (1991) determined empirically that the minimum lifetime for its chemical conversion to H_2O is of the order of 3 to 4 months at low latitudes in the upper stratosphere or somewhat longer than the time constants for meridional transport. Holton and Choi (1988) and Stanford et al. (1993) used the three-years of SAMS CH_4 data as a tracer for the characterization of the vertical and meridional components of the seasonal net transport. The present analysis study makes use of time series of CH_4 mixing ratio data as a function of pressure-altitude for 1992–2005 from the Halogen Occultation Experiment (HALOE) aboard the Upper Atmosphere Research Satellite (UARS). While not ideal, atmospheric sampling via solar occultation is adequate for obtaining the large-scale variations of CH_4.

The HALOE instrument obtained sunrise and sunset profiles of CH_4 in the stratosphere and lower mesosphere, and a number of researchers have made use of its CH_4 data for studies of middle atmosphere transport. Ruth et al. (1997), Randel et al. (1998), and later Shu et al. (2013) used the multi-year distributions of the HALOE CH_4 mixing ratio as a tracer for the effects of semi-annual oscillation (SAO) and quasi-biennial oscillation (QBO) forcings. Youn et al. (2006) analyzed time series of CH_4, H_2O, and HF from HALOE for their trends at 10 hPa and at one latitude zone, 40 to 45°, and they found differences for their trends between the two hemispheres. They related the trends that they found for the Northern Hemisphere to an intensification of stratospheric wave activity over that 14 yr time span.

2 Objectives and analysis approach

The present study is an analysis of time series of the HALOE CH_4 for an increasing trend in the subtropical ascent and for a correspondingly increasing trend in the extratropical descent in the same hemisphere. Multiple linear regression (MLR) techniques are used for the analyses, and they fit the seasonal and the interannually-varying forcings along with the trend terms in time series of CH_4 as a function of pressure-altitude.

ACPD
14, 24183–24220, 2014

Specifically, CH_4 time series are considered for separate subtropical and extratropical latitude zones of each hemisphere, as depicted in the simple schematic of Plumb (2007, Fig. 13). The coefficients of the trend terms and their statistical significance are given and discussed in Sect. 3 for the separate latitude zones and as a function of pressure-altitude.

Trends from analyses of the HALOE H_2O are shown in Sect. 4 and compared with those from CH_4 for consistency, since H_2O is the primary chemical product of the CH_4 oxidation at the upper altitudes. Section 4 also relates the time series of residuals from the analysis of CH_4 in the lower mesosphere to the de-seasonalized variations in HCl, another tracer-like molecule for the stratosphere and mesosphere. In particular, it is shown that the residuals from the separate MLR fits to the CH_4 and HCl series have small, irregular variations of opposite sign. It will be posited that the somewhat anomalous variations in the multi-year time series of HALOE HCl for the lower mesosphere that have been analyzed and reported by others are due to effects from non-periodic, wave forcings during 1992–2005. Section 5 is a summary of findings from the present analyses.

The effects of the seasonal, net circulation are apparent from monthly, zonal-mean cross sections of CH_4, as shown by Holton and Choi (1988) from the SAMS data and by Randel et al. (1998) and Shu et al. (2013) from the HALOE data. Qualitatively, there is a net upward transport of CH_4 at the low latitudes, a net poleward transport throughout the stratosphere, plus a descent of CH_4-poor air within the polar vortex beginning at upper altitudes (cf., Fig. 2). The monthly CH_4 distributions also often exhibit a significant mixing ratio gradient from the subtropics to higher latitudes along pressure surfaces in the middle and upper stratosphere. The exact latitude location of the maximum gradient varies seasonally, most likely according to the amount of meridional mixing of the air masses that occurred in the weeks before. The latitude vs. pressure-altitude images of HALOE CH_4 at the HALOE Website (http://haloe.gats-inc.com/home/) for October of successive years indicate that the net vertical transport of the CH_4 was suppressed during 1991, 1993, 1995, 1997, 1999, and 2004, while it was elevated in 1992, 1994,

ACPD
14, 24183–24220, 2014

1998, 2002, and 2003. Net effects for 1996, 2000, and 2001 are intermediate to those of the other years. Shu et al. (2013) showed that the strength or upward extent of the net circulation is related to the phase of the QBO and/or to the effects of the Rossby-wave forcing. To first order, the isolines for CH_4 in Fig. 2 and in the HALOE data also indicate that there are distinct BDC branches in the Northern Hemisphere and in the Southern Hemisphere. The sense of that net circulation is upward in the tropics and subtropics and downward in the extratropics.

Points for the data time series of the present study are generated using the HALOE version 19, Level 2 CH_4 profiles from occurrences of the HALOE sunrise (SR) or sunset (SS) tangent-point observations within a latitude zone for 1992–2005, as in Remsberg (2008). The SR and SS profiles are binned into extratropical ($55 \pm 15^{\circ}$) and subtropical ($14 \pm 14^{\circ}$) zones for the southern and the Northern Hemispheres and at 12 pressure-altitudes, giving a total of 48 separate time series for analysis. Example time series for the southern and northern extratropics are shown in Fig. 3a and b at 7 hPa (near 35 km). Each data point in Fig. 3 is an approximate snapshot of the zonally-averaged CH_4 for the latitude zone (cf., Fig. 2). The oscillating curves in Fig. 3 are the MLR fits to the data points from mid-1992 onward and based on the terms indicated at the lower left of the figure. The near horizontal line is the sum of the constant and linear trend terms. Data in the first year following the Mt. Pinatubo eruption of June 1991 often appear to have been perturbed and are not included for the MLR fittings. Initial analyses indicated that the only significant periodic terms for the extratropics are SAO, annual oscillation (AO), and QBO. Generally, a QBO term of 28 month (or 853 day) period is dominant in each data series. An additional term is added for the subtropical time series, having a period of 21 months (or 640 days) and labeled IA, or analogous to a modulation of the AO and QBO terms (Dunkerton, 2001). A gap of 12° in latitude is imposed between the adjacent edges of the extratropical and subtropical bins to minimize effects of the rather large meridional gradients in CH_4 that may occur between the two zones. Otherwise a term for the variation of CH_4 with latitude must be considered in the MLR models. Lag-1 autocorrelation (AR-1) effects are a significant part of the

ACPD
14, 24183–24220, 2014

MLR models. The accounting for AR-1 effects corrects for minor biases between the MLR model and the CH_4 points that may occur within short segments of a data series.

Nedoluha et al. (1998) reported that solar cycle (SC) effects on CH_4 are very small even near the stratopause; thus, no 11 yr or SC-proxy term was included in the MLR models. However, there is a cooling of the middle atmospheric during this 14 yr time span, due to the increasing atmospheric CO_2. Therefore, the analyses are conducted for time series of the CH_4 mixing ratio at pressure-altitudes rather than geometric altitudes. In this way, the added effects from the contraction of a pressure surface with altitude and time are avoided. To first order then, the variations of CH_4 with time at a pressure level represent the effects of the net diabatic transport both vertically within a zone and horizontally to adjacent latitude regions.

Compare the time series of Fig. 3 for the two extratropical zones. Their variations with time may be interpreted qualitatively with the aid of Fig. 2 showing the nominal distribution of CH_4. One can see that the amplitudes of the seasonal terms are different for the two hemispheres. The effects of the SAO and the AO are clear in the Southern Hemisphere in Fig. 3a, where the variations are mainly a result of a radiative relaxation from the effects of the net seasonal heating rather than from the effects of Rossby-wave forcings. The MLR seasonal cycle has its maximum in late autumn, and the constant term has a mean mixing ratio of 0.72 ppmv. Minimum data values of about 0.5 ppmv are apparent for some years in the south and most often in late winter, but they are not fit well by the model. They occur when the measurements for this zone extend into the polar vortex region, where the wintertime diabatic circulation is transporting low values of CH_4 downward. Figure 3b shows that a seasonal maximum occurs in late autumn to early winter in the northern extratropics, and its minimum is in late summer. The combined effects of the SAO and AO are of smaller amplitude in the north and appear to be blended compared with the southern extratropics (cf., Fig. 3a), perhaps due to meridional mixing of the air in the north at this pressure-altitude. Its mean mixing ratio is 0.66 ppmv or a bit lower than in the southern extratropics. Trend coefficients are

ACPD
14, 24183–24220, 2014

slightly positive in the south but negative in the north, and that difference is discussed in Sect. 3.

The corresponding CH_4 time series at 7 hPa are shown for the two subtropical zones in Fig. 4. Periodic variations in Fig. 4a for the Southern Hemisphere are primarily from the annual and QBO cycles; its average CH_4 is about 1.1 ppmv. Effects from the SAO term are not clearly apparent until the upper stratosphere (not shown). The data for the northern subtropics in Fig. 4b indicate a seasonal cycle that is weaker than in the south; interannual effects (QBO and IA) are present, too. There are also occasional data points that appear as low outliers in winter. In general, there is less periodic structure in the CH_4 of the northern subtropics at this level, most likely because of the mixing effects from the dissipation of Rossby waves and gravity waves. The mixing of air from the middle latitudes is likely responsible for the occurrence of the occasional, low wintertime data values. Trend coefficients are weakly positive in both hemispheres. At this point it is also noted that changes in the net circulation based on the CH_4 variations in the southern subtropics may also be affected some by the extratropical wave forcings of the Northern Hemisphere (see also Sect. 3).

Another example time series is shown in Fig. 5 for the northern subtropics at 30 hPa. The dominant periodic term in the data is a weak annual cycle, whose wintertime minimum reflects the effect of a mixing with older air from the extratropics. A weak QBO-like term is also present in the data, and the mean mixing ratio is 1.43 ppmv. This region ought to be affected most by the air that ascended from the tropical upper troposphere to the mid-stratosphere several years earlier. Tropospheric CH_4 was increasing from 1990–2003 at an average rate of 0.3 % yr^{-1} (or 3 % $decade^{-1}$) (Dlugokencky et al., 2009). The linear trend term from the MLR model is increasing and at a rate of 3.7 ± 2.6 % $decade^{-1}$ or essentially equal to that of the tropospheric CH_4. Trends in the CH_4 time series at higher altitudes are interpreted as indicating a change in the strength of the BDC, when they are positive and significantly larger than 3 % $decade^{-1}$ or significantly smaller than 3 % $decade^{-1}$ or even negative.

ACPD
14, 24183–24220, 2014

The retrieved HALOE CH_4 mixing ratios in Fig. 5 are only of order 1.2 ppmv in late 1991. Such low values may have been affected by a slight bias error in the lower stratosphere at that time, due to a reduced accuracy for the measured and retrieved CH_4 in the presence of the aerosol layer following the eruption of Mt. Pinatubo. However, Thomason (2012) reported that HALOE CH_4 does not appear to be affected by contamination from other minor or trace species from its retrieval algorithm, at least after that early volcanic period. The present study considers data points from mid-1992 and onward in the MLR analyses at all latitudes and pressure-altitudes, primarily to avoid contaminating effects in the lower stratosphere and/or anomalous net transport effects at higher altitudes for some months following the eruption.

3 Linear trends in CH_4

Time series of CH_4, like those in Figs. 3 through 5, are analyzed at 55° S, 14° S, 14° N, and 55° N. Table 1 contains the mean mixing ratio profiles of CH_4 from the constant terms for each of the four latitude zones. The mean mixing ratio profiles show very good symmetry between the two hemispheres for the subtropics; there is also more CH_4 in the subtropics than in the extratropics for both hemispheres. In the middle to lower stratosphere there is slightly more CH_4 in the southern than in the northern extratropics, an indication that the net wintertime descent is prolonged and/or a bit stronger in the north. At 50 hPa the mixing ratios are very nearly identical between the two hemispheres for the subtropics (1.52 ppmv) and for the extratropics (1.22 ppmv), indicating that the tropospheric CH_4 that entered the lowest part of tropical stratosphere was transported poleward and mixed about equally with the higher latitude air. There is also a monotonic decrease of the CH_4 with altitude in each latitude zone, due to the chemical oxidation of CH_4 to H_2O. The mean CH_4 mixing ratio profiles in Table 1 represent qualitatively the effects of the seasonal BDC transport within each hemisphere.

The conceptual idea of Plumb (2007, Figs. 13 and 15) for an acceleration of the hemispheric BDC from a species like CH_4, whose mixing ratio decreases with altitude

ACPD
14, 24183–24220, 2014

as in Fig. 2, is indicated here by trends that are positive by more than 3 % decade^{-1} in the subtropics, but more weakly positive (or negative) in the extratropics. Thus, an acceleration of the BDC leads to a higher CH_4 value in the subtropics and a lower value in the extratropics or a steepening of its Equator-to-Pole gradient with time for a given pressure-altitude. On the other hand, the effects of meridional mixing can transport extratropical air back to the subtropical zone and cause a net recirculation of CH_4 (Garny et al., 2014). It is not possible to quantify those separate effects based on the CH_4 observations alone. The analyzed trend terms (% decade^{-1}) and the accompanying confidence intervals or CI (in %) that they are present in the time series are given in Table 2. The trend terms indicate only where there is an acceleration of the overall net circulation. Note that the highly significant trends are shown by boldface type; they have a CI equal to or greater than 95 % of being present in the time series. The trend coefficients of the low to middle stratosphere are generally significant in the northern but not the Southern Hemisphere. It is noted that some of the relatively large trends for the CH_4 time series of the upper stratosphere also carry fairly small uncertainties from the MLR analysis, but those trends are not highly significant because there is non-periodic structure in the time series of their residuals that has not been accounted for. Checking for structure in the residuals is an important part of the MLR analysis.

Figure 6 is a plot of the trend profiles in % decade^{-1} from Table 2 for the subtropics and the extratropics of the Southern Hemisphere. Their 2σ uncertainties are shown as horizontal bars at selected levels, and the only highly significant trends are in the subtropics at 7 hPa or 7.0 (2.2) and at 10 hPa or 4.0 (2.2). The vertical dashed line represents a trend of 3 % decade^{-1} or equivalent to that of the tropospheric CH_4. First, it appears that the shallow branch of the BDC may have experienced a deceleration at 30 and 20 hPa (or a negative trend in the subtropics and a positive trend in the extratropics). Those trends are not highly significant, however. The trends in the middle stratosphere are positive in both the subtropics and the extratropics, and the subtropical trends are significant. Yet, their signs disagree with the conceptual picture for an acceleration of the BDC. The trends around the stratopause (1 hPa) are larger, and

ACPD
14, 24183–24220, 2014

they carry the correct signs for an acceleration of the BDC – larger and positive in the subtropics and large and negative in the extratropics. Still, it is stressed that none of those upper level CH_4 trend terms are highly significant.

Figure 7 is a plot of the subtropical and extratropical trend profiles from Table 2 for the Northern Hemisphere. The highly significant, northern subtropical trends and their 2σ uncertainties are 4.5 (2.6) at 10 hPa, 6.7 (2.5) at 20 hPa, 3.7 (2.6) at 30 hPa, and 2.9 (2.8) at 50 hPa. Significant trends for the northern extratropics are −7.9 (3.9) at 7 hPa, −12 (2.6) at 10 hPa, 2.5 (3.0) at 30 hPa, and 3.8 (2.2) at 50 hPa. The trends at 50 and 30 hPa vary within 2.5 to 3.8 % decade^{-1}, but they carry the same sign and disagree with the picture of an acceleration of the net circulation or BDC. Instead, they are consistent with the average trend of 3 % decade^{-1} for the tropospheric CH_4, and they indicate that the trends in the extratropics are merely reflecting a net transport of tropical air to the higher latitudes. The CH_4 trends from 20 hPa to 7 hPa are larger and positive in the subtropics, and the corresponding extratropical trends are increasingly negatively up to 10 hPa and remain negative even at 7 hPa. Thus, the signs of the trends from those two northern zones imply that there was an acceleration of the BDC in the middle stratosphere. In other words, an acceleration is indicated during this time span for the lower part of the deep branch or for an upward extension of the shallow branch of the BDC.

Youn et al. (2006) obtained a positive linear trend at 10 hPa of 9 % decade^{-1} at 42.5° S, but almost no trend at 42.5° N. For comparison purposes, linear trends were also calculated at 10 hPa for the same latitude zones of 40 to 45° in each hemisphere. Those trends are 8.6 % decade^{-1} in the southern and −9.4 % decade^{-1} in the Northern Hemisphere. A primary reason for the differing results for the Northern Hemisphere is that the MLR model of the present study includes periodic terms and the effects of autocorrelation among all terms. The trends for the wider latitude zones herein are 4.8 % decade^{-1} in the south and −12 % decade^{-1} in the north (Table 2).

A change for the BDC may not be as easy to determine for the upper stratosphere because the photochemical lifetime for the conversion of CH_4 to H_2O is comparable to

ACPD
14, 24183–24220, 2014

the time constant for the net transport. The trends in Fig. 7 are small (−1.9 % decade^{-1}) and not significant at 2 hPa in the northern subtropics. This result is inconsistent with the decreasing trends for CH_4 at low latitudes reported by Nedoluha et al. (1998, their Fig. 1) for the time span of 1991–1997. As a check, a selected re-analysis of the HALOE data was carried out for their latitude zone of 10° S to 10° N, but for the entire time period of 1991–2005; the MLR fit to that particular time series is shown in Fig. 8. Qualitatively, the structure in the respective time series is the same from late 1991 to early 1997. Yet, Fig. 8 indicates that the HALOE CH_4 exhibits a peak value of order 0.9 ppmv in the spring of 1997 or equivalent to the value in early 1992. Thus, if Nedoluha et al. (1998) had extended their time series for another six months or so, they should not have found a decreasing trend for the HALOE CH_4.

Table 2 and Fig. 7 show a negative trend (−5.7 % decade^{-1}) at 1 hPa in the northern subtropics, indicating that there may have been a deceleration of the net circulation at the uppermost levels of the deep branch of the BDC. Even so, that negative trend is not highly significant because its time series residuals have non-periodic structures that are unaccounted for (see also Sect. 4). The role of changes in the wave forcing on the net circulation is more complicated near the tropical stratopause. It depends on the altitude region for the wave dissipation, as well as effects of the meridional transport and mixing on the CH_4. In support of that prospect, Randel et al. (2000) reported that there was a minimum in stratospheric wave forcing for the years 1993–1997, followed by an increase in 1998–1999. An inspection of the latitude vs. pressure-altitude cross sections of CH_4 at the HALOE Website indicates that the seasonal BDC (as defined by the character of its monthly CH_4 distributions) extends to higher altitudes in the northern than in the Southern Hemisphere in the early and middle 1990s than for later in the time series (cf., September/October distributions for 1992 and 1994 with those of 1999 and 2002). It is noted that those annual differences are modulated by the phase of the QBO; however, a QBO term is included in the present MLR models, and it fits those oscillations well. Apparent negative trends in Fig. 7 are present from 3 to 0.7 hPa for the northern subtropics, where secondary residual circulations associated with the descent

ACPD
14, 24183–24220, 2014

of the SAO or with stratospheric warming events are often pronounced (Hitchman and Leovy, 1986). For example, the qualitative effect during and just following a warming event is to enhance meridional transport of a tracer (like CH_4) in the upper stratosphere and mesosphere. Pawson and Naujokat (1999) recorded no midwinter warming events for the Northern Hemisphere in the middle 1990s; Manney et al. (2005) reported that midwinter warming events were more prevalent after that. Thus, it may be that the subtropical trend profiles are merely reflecting the effects of changes in stratospheric wintertime warming activity during 1992–2005, rather than representing any longer-term trend for a change of the deep branch of the BDC at those upper levels. Such dynamical forcings would tend to be of large amplitude, but somewhat episodic, and they may explain most of the structure that is present in the MLR model residuals for the upper stratosphere and lower mesosphere of the Northern Hemisphere.

4 Trends in H_2O and HCl

Supporting evidence is sought from the concurrent trends in HALOE H_2O. Trend profiles are obtained from HALOE H_2O using the same terms that were applied in the MLR models for CH_4, and the results are compared for the extratropics in Figs. 9 and 10. First, it is noted that the mean mixing ratio profiles for H_2O are nearly symmetric for each latitude zone between the two hemispheres (not shown). H_2O values for the subtropics increase from about 3.9 ppmv at 50 hPa to about 6.2 ppmv at 0.3 hPa. H_2O increases in the upper stratosphere from the subtropics to the extratropics, due mostly to the oxidation of CH_4 to H_2O and to its net transport poleward. To first order, half of the H_2O in the upper stratosphere and lower mesosphere is the result of the chemical oxidation of CH_4 to H_2O, and the sum of $2CH_4 + H_2O$ is nearly conserved (Brasseur and Solomon, 2005). Therefore, it is expected that the trends for CH_4 vs. those for H_2O will have a 2 : 1 ratio at those altitudes but be opposite in sign. The remaining part of the H_2O trend in the lower mesosphere is from the H_2O that entered the stratosphere through the tropical tropopause, where the air has an H_2O mixing ratio of about

ACPD
14, 24183–24220, 2014

3.5 ppmv. Seasonally-varying, entry-level values have been reported for the HALOE H_2O of the lower stratosphere (see Randel et al., 2006). Therefore, the H_2O and CH_4 trends are shown for the extratropics only, and the H_2O trends are not plotted for the lower stratosphere.

The trend terms for H_2O are highly significant in the extratropics of the Southern Hemisphere from 2 hPa to 0.3 hPa in Fig. 9. The trends for CH_4 in that altitude region also have a fairly high CI of between 73 and 92 %, and they vary from −8.4 to −11 % in Fig. 6 (and in Table 2). The trends for H_2O are opposite in sign and vary between 3.0 and 4.6 % in Fig. 9 and are in good accord with expectations from the methane oxidation chemistry. The respective trends for the extratropics of the Northern Hemisphere also have opposing signs, but their magnitudes do not agree as well with the simple estimates from the conversion of CH_4 to H_2O (cf., Figs. 7 and 10).

Trends in H_2O in the middle stratosphere in Fig. 9 are slightly negative in the southern extratropics and they are more negative in the subtropics (not shown). This finding reflects changes for the H_2O entering the stratosphere during 1992–2005. In fact, Randel et al. (2006) reported observing a sharp decrease in HALOE H_2O in 2001 that persisted through 2005, and they ascribed that decrease to a change in the BDC near the tropopause. The linear trends for H_2O from the current study are also negative and highly significant at 50 hPa and at most other levels of the lower stratosphere. However, there are large differences in the H_2O trends at 7 and 10 hPa across the two subtropical zones of each hemisphere (cf., Figs. 9 and 10), indicating differences for the net transport within the hemispheres. Further, the H_2O trend in the Northern Hemisphere at 5 hPa is positive and highly significant or 4.6 (0.3) % decade^{-1}. Taking into account the age-of-air for 55° N, that finding agrees with the long-term trend of about 6 % decade^{-1} that was reported as representative of H_2O for the years prior to 2001 (Scherer et al., 2008).

To summarize the joint findings from CH_4 and H_2O, the trends from CH_4 are significant and of the correct sense for a speed-up of the BDC at pressure-altitudes of 20 to 7 hPa in the Northern Hemisphere. Conversely, there is no clear evidence for

ACPD
14, 24183–24220, 2014

a change in the BDC in the Southern Hemisphere, except perhaps for the extratropics of the lower mesosphere. The weakly positive CH_4 trends of the lowest part of the stratosphere (or below the 20-hPa level) are merely indicative of the slow increases of tropospheric CH_4 during 1992–2005. The concurrent trends for CH_4 and H_2O are highly significant in the lower stratosphere of the Northern Hemisphere, but the trend for H_2O is judged as mainly a result of the episodic change in 2001 for the entry-level H_2O. The H_2O trends for the middle stratosphere are negative in the southern but not in the Northern Hemisphere, most likely because of a more vigorous meridional mixing of the air masses in the Northern Hemisphere. Together then, the trends from both CH_4 and H_2O indicate that the low altitude part of the deep branch of the BDC underwent an acceleration up to near 7 hPa in the Northern Hemisphere during 1992–2005.

Figure 11 is the MLR model fit to the CH_4 time series data at 0.7 hPa of the northern extratropics and subtropics. Note that the IA term is not important at 0.7 hPa and is excluded in the subtropical MLR model of Fig. 11. The extratropical minimum occurs in late summer, due to the nearly complete oxidation of the CH_4 at that time. Conversely, there is a maximum in the subtropics in late summer in response to the diabatic circulation associated with the radiative relaxation away from the very warm temperatures of the polar summer stratopause. Upon closer inspection, one can readily see that these predominant, annual cycle variations in the data of the extratropics are underestimated by the MLR model terms in 1992, in 1998–1999, and in 2003–2005 and overestimated in 2000 and 2001. The late summer maximum of the subtropics is overestimated by the model in 1996 and in 2000–2001; the model also clearly underestimates the data in the winter of 1997–1998. Occasional seasonal amplitude anomalies are also present in the CH_4 analysis for the southern subtropics, but are nearly absent in the southern extratropics (not shown). Of course, the seasonal terms of the MLR model simply provide an average fit to the data across all the years. Thus, the time series of HALOE CH_4 of the Northern Hemisphere indicate that there must be a connection to effects from aperiodic dynamical forcings. It ought to be possible to verify those instances of

ACPD
14, 24183–24220, 2014

MLR/data mismatch with the aid of a model study for a CH_4-like tracer, transported with the aid of assimilated temperature and ozone fields for those years.

A number of investigators have analyzed time series of HCl in the lower mesosphere to verify concurrent changes in the effects of reactive chlorine on ozone (e.g., Froidevaux et al., 2006). HCl is the primary product of the chemical conversion of free chlorine from methyl chloride and from CFC molecules in the upper stratosphere (Brasseur and Solomon, 2005). For this reason HCl may also be considered as a tracer-like species for studying transport and age-of-air, particularly for the uppermost stratosphere and lower mesosphere. Model studies show peak values of HCl occurring in the lower mesosphere in 1999, while the HCl time series from HALOE at 0.46 hPa and up to 2001 indicated that the observed maximum occurred a year of two earlier or in 1997 (e.g., Waugh et al., 2001). However, the complete time series of HALOE HCl shows two maxima – one in 1997 and another from 2001–2002 (WMO, 2007, Figs. 1–12). It may be that there were significant variations in the observed HCl due to dynamical forcings at those altitudes, and the transport models do not represent them so well. The MLR models of the present study are fitting the periodic terms in the observed data fairly well. But as indicated in the CH_4 time series of Fig. 11, some forcing effects are not periodic. In particular, major stratospheric, midwinter warming events can alter the distributions of tracers, but not in the same way each year and perhaps not every winter. Further, the usual method of de-seasonalizing a data time series can also impart significant structure to the MLR model residuals.

Spatial gradients for CH_4 and HCl in the lower mesosphere are opposite in sign both vertically and in the meridional direction, such that any anomalies in their respective residuals should have opposing features that would tend to confirm effects from dynamical forcings. Therefore, MLR analyses are applied to time series of both CH_4 and HCl in the lower mesosphere. As shown in Fig. 11, CH_4 has seasonal and QBO-like forcings that are resolved and accounted for reasonably well with the MLR models; the same terms are applied to the HALOE HCl time series. A quadratic term is also added to the linear term for the HCl MLR model because HCl varied non-linearly dur-

ACPD
14, 24183–24220, 2014

ing 1992–2005. Figure 12 shows time series of the residuals (data minus MLR model curve) for HCl in the northern extratropical zone at 0.7 hPa (near 52 km). In general, the residuals indicate a good fit to the data, although they tend to be mostly negative from late 1998 through 1999 and mostly positive in 1995–1996 and in 2001. Figure 13 shows the corresponding residuals for CH_4; they indicate little to no bias from 1992 to mid-1999, but then a clear negative bias in 2000 and 2001, or opposite to that from HCl. Thus, there is aperiodic structure remaining in the residuals for both HCl and CH_4, and their opposing signs indicate that the net circulation at this level is being altered by dynamical forcings. In fact, it should be clear that one ought to achieve more consistent HCl model/data comparisons by analyzing time series of the HCl within a latitude zone but referenced to a constant CH_4 level instead of to an altitude or even a pressure level. A corollary is that it is important to know how well a given chemistry/climate model is able to simulate the observed time series of the CH_4, too. Further, it should be possible to extend the HALOE CH_4 and HCl time series by considering data from the Atmospheric Chemistry Experiment (ACE), which began providing operational data early in 2004 (Bernath, 2013) and/or data from the Michelson Interferometer for Passive Atmospheric Sounding (MIPAS) that began operations in 2002 (Fischer and Oelhaf, 1996).

5 Conclusions

Time series of the tracer-like molecule CH_4 obtained with the UARS HALOE experiment are analyzed using MLR techniques for their periodic and trend terms during 1992–2005. The sunset and sunrise profile data are binned according to subtropical and extratropical latitude zones in both the southern and Northern Hemispheres. Time series are generated and analyzed from 50 to 0.4 hPa. Based on an examination of the data time series, both seasonal and interannual terms are included in the MLR models, in addition to a linear trend term. The trend terms are examined to see whether there had been any change in the net circulation for the southern or Northern Hemispheres during 1992–2005 in accordance with the simple concept of Plumb (2007) for a hemi-

ACPD
14, 24183–24220, 2014

spheric BDC. The adoption of that concept suggests that an acceleration of the circulation is indicated whenever the CH_4 trends are positive by more than 3 % decade^{-1} in the subtropics and less than that or negative in the extratropics. Further, since the analyses are conducted at pressure levels rather than at geometric altitudes, it is presumed that any significant trends must be due mainly to changes in the effects of wave forcings on the distributions of CH_4.

The primary findings of this study are as follows. The CH_4 trend terms for the Northern Hemisphere are significant from 50 to 7 hPa. They are positive in the subtropics and larger than the tropospheric CH_4 trends of about 3 % decade^{-1} from 20 to 7 hPa. In the northern extratropics the trends are clearly negative at 10 and 7 hPa. At those levels the overall trend signature across those two zones represents an acceleration of the BDC for the Northern Hemisphere. The CH_4 trends are positive and significant at 7 and 10 hPa for the southern subtropics, but the corresponding trends in the southern extratropics are also positive; thus, their combination is not in the proper sense for indicating an acceleration or deceleration of the southern hemispheric BDC. CH_4 trends are not highly significant for the stratosphere above the 7-hPa level in either zone of both hemispheres. The early climate model simulations of Rind et al. (1990) are qualitatively consistent with these findings, in that their model runs show more wave activity and dissipation throughout the winter in the northern than in the Southern Hemisphere for their model scenario of steady increases of CO_2 in the atmosphere. Still, it may be that estimates of the net circulation from HALOE are only representative of 1992–2005.

The trends for HALOE H_2O are compared for the extratropics with those from CH_4 in the upper stratosphere and lower mesosphere because H_2O is the primary product of the oxidation of CH_4 at those altitudes. An approximate inverse and 2 : 1 relationship between their trends (CH_4 : H_2O) is found near the stratopause in both hemispheres, but that result is most significant in the Southern Hemisphere. Trends for HALOE H_2O in the low to middle stratosphere are large and significant, but they reflect mainly the episodic change in 2001 for the entry of H_2O into the stratosphere from below.

ACPD
14, 24183–24220, 2014

The variation of CH_4 with time in the lower mesosphere also provides some clues about the effects of aperiodic wave forcings in the lower mesosphere. Others have noted that there are modest disagreements in the modeled trends for HCl compared to those observed with HALOE, particularly from about 1996 to 2002. But both CH_4 and HCl should serve as tracers of changes due to dynamical forcings. It is shown that their respective time series residuals are anti-correlated. A part of the anomalies in the CH_4 residuals is due to the significant variations in the seasonal amplitudes of the observed CH_4, and they are ascribed to wave-driven, secondary residual circulations associated with the SAO and QBO. Therefore, a better approach would be to analyze for trends in HCl as referenced to constant CH_4 values. In summary, it is concluded that near-global distributions of CH_4, as remotely measured from a satellite, are an excellent diagnostic of the effects of seasonal and longer-term changes in the transport within the middle atmosphere.

Acknowledgements. Figure 1 is attributed to Ted Shepherd, Doug Degenstein, and the Optical Spectrograph and InfraRed Imager System (OSIRIS) satellite experiment Team. Figure 2 was kindly provided by Eric Fleming of SSAI and NASA Goddard. The author (EER) carried out this work while serving as a Distinguished Research Associate within the Science Directorate at NASA Langley.

References

Bernath, P. F. (ed.): The Atmospheric Chemistry Experiment ACE at 10: A Solar Occultation Anthology, A. Deepak Publ., Hampton, Virginia, 532 pp., 2013.

Brasseur, G. and Solomon, S.: Aeronomy of the middle atmosphere, 3rd Edition, in Atmospheric and Oceanographic Sciences Library, vol. 32, Springer, the Netherlands, 644 pp., 2005.

Butchart, N.: The Brewer–Dobson circulation, Rev. Geophys., 52, 157–184, 2014.

Dlugokencky, E. J., Bruhwiler, L., White, J. W. C., Emmons, L. K., Novelli, P. C., Montzka, S. A., Masarie, K. A., Lang, P. M., Crotwell, A. M., Miller, J. B., and Gatti, L. V.: Observational constraints on recent increases in the atmospheric CH_4 burden, Geophys. Res. Lett., 36, L18803, doi:10.1029/2009GL039780, 2009.

ACPD
14, 24183–24220, 2014

Dunkerton, T. J.: On the mean meridional mass motions of the stratosphere and mesosphere, J. Atmos. Sci., 35, 2325–2333, 1978.
Dunkerton, T. J.: Quasi-biennial and subbiennial variations of stratospheric trace constituents derived from HALOE observations, J. Atmos. Sci., 58, 7–25, 2001.
Fischer, H. and Oelhaf, H.: Remote sensing of vertical profiles of atmospheric trace constituents with MIPAS limb emission spectrometers, Appl. Opt., 35, 2787–2796, 1996.
Fleming, E. L., Jackman, C. H., Stolarski, R. S., and Considine, D. B.: Simulation of stratospheric tracers using an improved empirically based two-dimensional model transport formulation, J. Geophys. Res., 104, 23911–23934, 1999.
Froidevaux, L., Livesey, N. J., Read, W. G., Salawitch, R. J., Waters, J. W., Brouin, B., MacKenzie, I. A., Pumphrey, H. C., Bernath, P., Boone, C., Nassar, R., Montzka, S., Elkins, J., Cunnold, D., and Waugh, D.: Temporal decrease in upper atmospheric chlorine, Geophys. Res. Lett., 33, L23812, doi:10.1029/2006GL027600, 2006.
Garcia, R. R, Randel, W. J., and Kinnison, D. E.: On the determination of age of air trends from atmospheric trace species, J. Atmos. Sci., 68, 139–154, doi:10.1175/2010JAS3527.1, 2011.
Garny, H., Birner, T., Boenisch, H., and Bunzel, F.: The effects of mixing on age of air, J. Geophys. Res., 119, 7015–7034, doi:10.1002/2013JD021417, 2014.
Hitchman, M. H. and Leovy, C. B.: Evolution of the zonal mean state in the equatorial middle atmosphere during October 1978–May 1979, J. Atmos. Sci., 43, 3159–3176, 1986.
Holton, J. R. and Choi, W- K.: Transport circulation deduced from SAMS trace species data, J. Atmos. Sci., 45, 1929–1939, 1988.
Lin, P. and Fu, Q.: Changes in various branches of the Brewer–Dobson circulation from an ensemble of chemistry climate models, J. Geophys. Res., 118, 73–84, doi:10.1029/2012JD018813, 2013.
Manney, G. L., Zurek, R. W., O'Neill, A., and Swinbank, R.: On the motion of air through the stratospheric polar vortex, J. Atmos. Sci., 51, 2973–2994, 1994.
Manney, G. L., Krüger, K., Sabutis, J. L., Sena, S. A., and Pawson, S.: The remarkable 2003–2004 winter and other recent warm winters in the Arctic stratosphere since the late 1990s, J. Geophys. Res., 110, 1–14, doi:10.1029/2004JD005367, 2005.
Nedoluha, G. E., Siskind, D. E., Bacmeister, J. T., Bevilacqua, R. M., and Russell III, J. M.: Changes in upper stratospheric CH_4 and NO_2 as measured by HALOE and implications for changes in transport, Geophys. Res. Lett., 35, 987–990, 1998.

ACPD
14, 24183–24220, 2014

Okamoto, K., Sato, K., and Akiyoshi, H.: A study on the formation and trend of the Brewer–Dobson circulation, J. Geophys. Res., 116, D10117, doi:10.1029/2010JD014953, 2011.
Pawson, S. and Naujokat, B.: The cold winters of the middle 1990s in the northern lower stratosphere, J. Geophys. Res., 104, 14209–14222, 1999.
Plumb, R. A.: Tracer interrelationships in the stratosphere, Rev. Geophys., 45, RG4005, doi:10.1029/2005RG000179, 2007.
Plumb, R. A. and Ko, M. K. W.: Interrelationships between mixing ratios of long-lived stratospheric constituents, J. Geophys. Res., 97, 10145–10156, 1992.
Randel, W. J., Wu, F., Russell III, J. M., Roche, A., and Waters, J. W.: Seasonal cycles and QBO variations in stratospheric CH_4 and H_2O observed in UARS HALOE data, J. Atmos. Sci., 55, 163–185, 1998.
Randel, W. J., Wu, F., Russell III, J. M., Zawodny, J. M., and Nash, J.: Interannual changes in stratospheric constituents and global circulation derived from satellite data, in: Atmospheric Science Across the Stratopause, edited by: Siskind, D. E., Eckermann, S. D., and Summers, M. E., American Geophysical Union, Washington, DC, doi:10.1029/GM123p0271, 271–285, 2000.
Randel, W. J., Wu, F., Voemel, H., Nedoluha, G. E., and Forster, P.: Decreases in stratospheric water vapor after 2001: links to changes in the tropical tropopause and the Brewer–Dobson circulation, J. Geophys. Res., 111, D12312, doi:10.1029/2005JD006744, 2006.
Remsberg, E. E.: On the response of Halogen Occultation Experiment (HALOE) stratospheric ozone and temperature to the 11-yr solar cycle forcing, J. Geophys. Res., 113, D22304, doi:10.1029/2008JD010189, 2008.
Rind, D., Suozzo, R., Balachandran, N. K., and Prather, M. J.: Climate changes and the middle atmosphere. Part I: the doubled CO_2 climate, J. Atmos. Sci., 47, 475–494, 1990.
Ruth, S., Kennaugh, R., Gray, L. J., and Russell III, J. M.: Seasonal, semiannual, and interannual variability seen in measurements of methane made by the UARS Halogen Occultation Experiment, J. Geophys. Res., 102, 16189–16199, 1997.
Scherer, M., Vömel, H., Fueglistaler, S., Oltmans, S. J., and Staehelin, J.: Trends and variability of midlatitude stratospheric water vapour deduced from the re-evaluated Boulder balloon series and HALOE, Atmos. Chem. Phys., 8, 1391–1402, doi:10.5194/acp-8-1391-2008, 2008.
Shaw, T. A. and Shepherd, T. G.: Raising the roof, Nat. Geosci., 1, 12–13, 2008.
Shepherd, T. G.: Transport in the middle atmosphere, J. Meteorol. Soc. Japan, 85B, 165–191, 2007.

ACPD
14, 24183–24220, 2014

Shu, J., Tian, W., Hu, D., Zhang, J., Shang, L., Tian, H., and Xie, F.: Effects of the quasi-biennial oscillation and stratospheric semiannual oscillation on tracer transport in the upper stratosphere, J. Atmos. Sci., 70, 1370–1389, doi:10.1175/JAS-D-12-053.1, 2013.

Solomon, S., Kiehl, J. T., Garcia, R. R., and Grose, W.: Tracer transport by the diabatic circulation deduced from satellite observations, J. Atmos. Sci., 43, 1603–1617, 1986.

Stanford, J. L. and Ziemke, J. R.: CH_4 and N_2O photochemical lifetimes in the upper stratosphere: in situ estimates using SAMS data, Geophys. Res. Lett., 18, 677–680, 1991.

Stanford, J. L., Ziemke, J. R., and Gao, S. Y.: Stratospheric circulation features deduced from SAMS constituent data, J. Atmos. Sci., 50, 226–246, 1993.

Thomason, L. W.: Toward a combined SAGE II-HALOE aerosol climatology: an evaluation of HALOE version 19 stratospheric aerosol extinction coefficient observations, Atmos. Chem. Phys., 12, 8177–8188, doi:10.5194/acp-12-8177-2012, 2012.

Waugh, D. W., Considine, D. B., and Fleming, E. L.: Is upper stratospheric chlorine decreasing as expected?, Geophys. Res., Lett., 28, 1187–1190, 2001.

World Meteorological Organization: Scientific assessment of ozone depletion: 2006, Global Ozone Research and Monitoring Project, Report No. 50, Geneva, Switzerland, 2007.

Youn, D., Choi, W., Lee, H., and Wuebbles, D. J.: Interhemispheric differences in changes of long-lived tracers in the middle stratosphere over the last decade, Geophys. Res. Lett., 33, L03807, doi:10.1029/2005GL024274, 2006.

ACPD
14, 24183–24220, 2014

Table 1. Mean CH_4 mixing ratio profiles (ppmv).

P (hPa)	55° S	14° S	14° N	55° N
0.4	0.19	0.24	0.25	0.18
0.5	0.20	0.26	0.27	0.19
0.7	0.21	0.30	0.33	0.21
1.0	0.24	0.36	0.40	0.24
2.0	0.34	0.56	0.61	0.34
3.0	0.44	0.71	0.75	0.42
5.0	0.60	0.92	0.94	0.55
7.0	0.72	1.06	1.07	0.66
10.0	0.84	1.19	1.18	0.78
20.0	1.02	1.37	1.33	0.98
30.0	1.10	1.45	1.43	1.08
50.0	1.22	1.53	1.52	1.22

ACPD
14, 24183–24220, 2014

Table 2. CH_4 trend profiles (% decade^{-1}) and their confidence intervals (%) per latitude zone.

Pressure (hPa)	55° S	14° S	14° N	55° N
0.4	−8.4, 73	7.2, 2	8.0, 24	−15.0, 89
0.5	−10.0, 80	7.2, 2	5.5, 20	−16.0, 90
0.7	−11.0, 91	6.6, 2	−2.6, 36	−16.0, 90
1.0	−11.0, 92	5.2, 6	−5.7, 34	−14.0, 88
2.0	−6.3, 64	2.7, 18	−1.9, 33	−8.1, 78
3.0	−1.2, 19	8.2, 52	0.9, 16	−5.7, 72
5.0	3.5, 43	7.0, 88	6.7, 48	−4.7, 89
7.0	4.3, 82	**7.0, 98**	4.7, 83	**−7.9, 97**
10.0	4.8, 93	**4.0, 98**	**4.5, 98**	**−12.0, 97**
20.0	5.0, 56	−0.3, 36	**6.7, 99**	−3.0, 68
30.0	2.1, 9	−1.1, 46	**3.7, 99**	**2.5, 95**
50.0	−0.5, 86	−1.2, 70	**2.9, 99**	**3.8, 99**

ACPD
14, 24183–24220, 2014

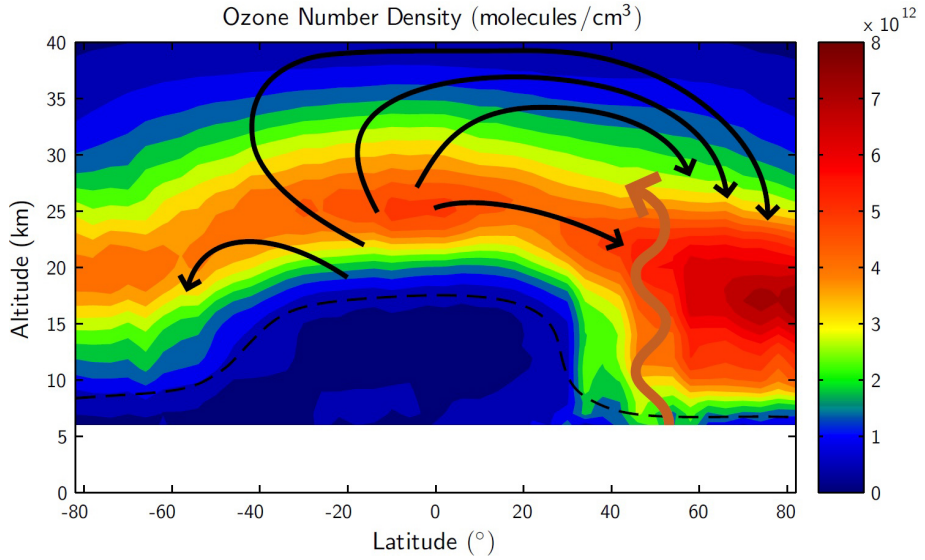

Figure 1. Brewer–Dobson circulation (BDC) and stratospheric ozone. The sense of this net circulation or BDC is shown by the black arrows overlain on the zonally-averaged ozone distribution (or its number density in molecules per cm^3 vs. latitude and altitude) for March 2004, as measured by the OSIRIS satellite instrument. Wiggly orange arrow indicates the propagation of waves from the troposphere as they affect the ozone. The dashed black line is the tropopause (adaption of figure in Shaw and Shepherd, 2008).

ACPD
14, 24183–24220, 2014

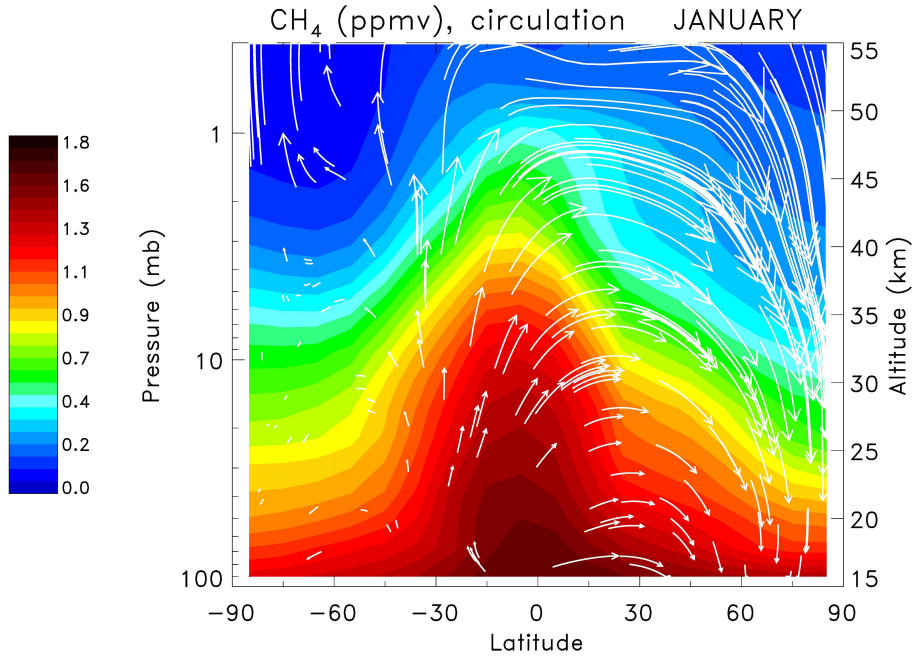

Figure 2. Methane distribution (ppmv) for January based on a chemistry and transport model simulation. White arrows indicate the sense and strength of the net circulation (image courtesy of Eric Fleming).

ACPD
14, 24183–24220, 2014

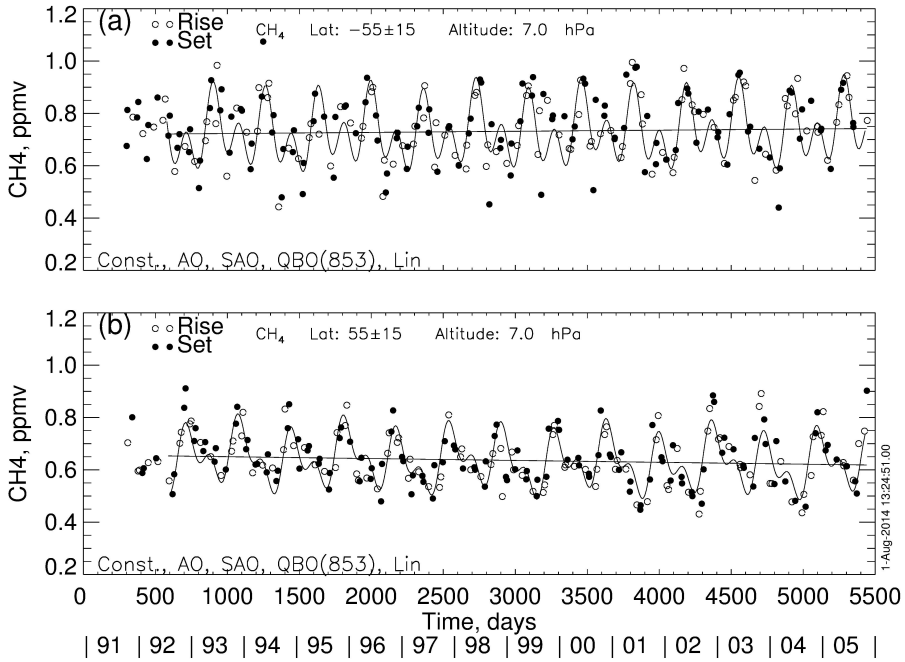

Figure 3. Time series of CH_4 is from HALOE at 7 hPa and for the extratropics of the **(a)** Southern and of the **(b)** Northern Hemisphere. Solid and open circles indicate the bin-averaged CH_4 data for sunset and sunrise, respectively. The oscillating curve is the MLR fit to the data based on the terms indicated at the lower left, and the near-horizontal line represents the sum of the constant and linear trend terms.

ACPD
14, 24183–24220, 2014

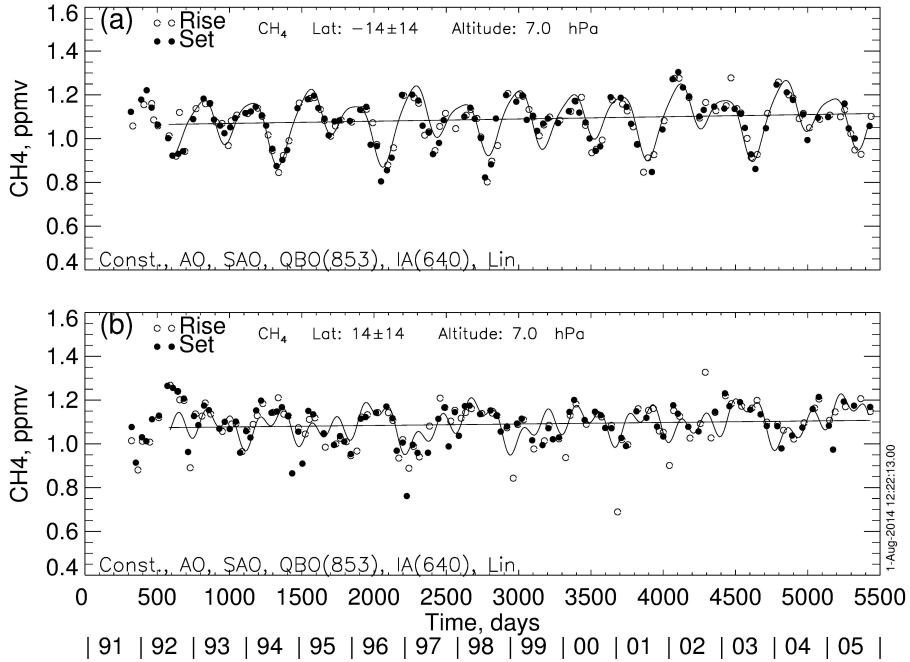

Figure 4. As in Fig. 3, but for the subtropics of the **(a)** Southern and of the **(b)** Northern Hemisphere.

ACPD
14, 24183–24220, 2014

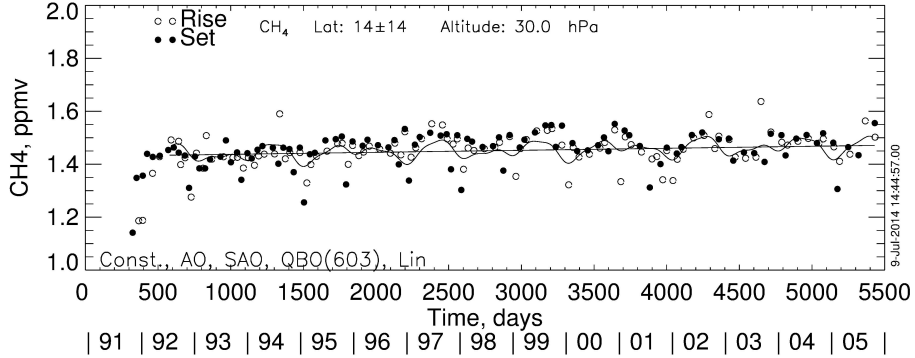

Figure 5. As in Fig. 3, but at 30 hPa for the subtropics of the Northern Hemisphere.

ACPD
14, 24183–24220, 2014

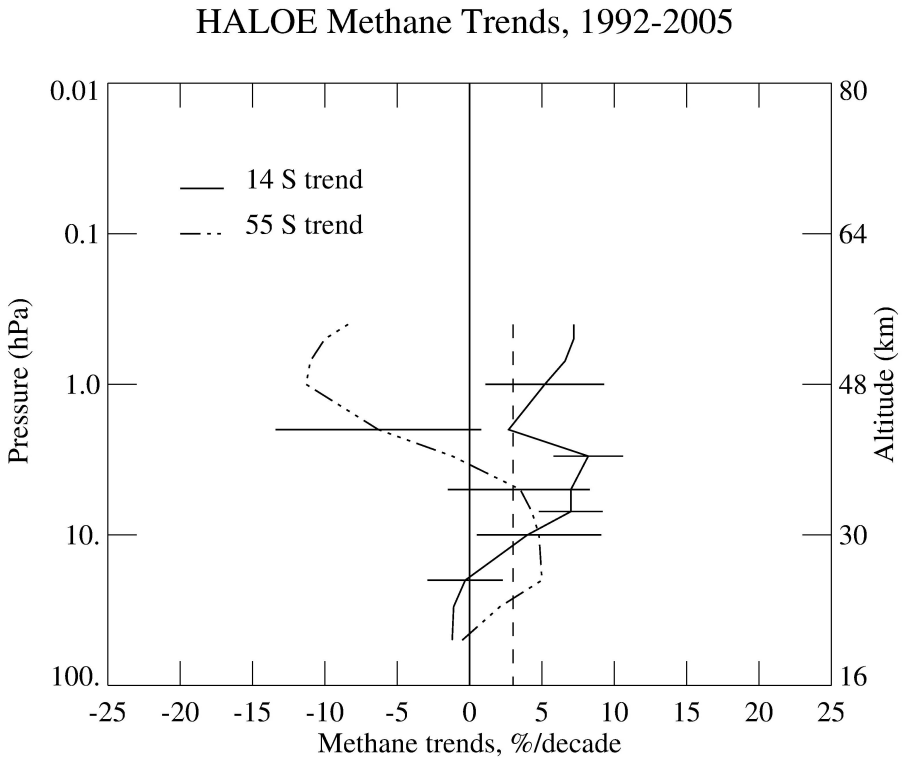

Figure 6. Subtropical and extratropical trend profiles for CH_4 in the Southern Hemisphere. Vertical dashed line is approximate trend for tropospheric CH_4. Horizontal bars at selected levels are the 2σ error estimates for the trend terms.

ACPD
14, 24183–24220, 2014

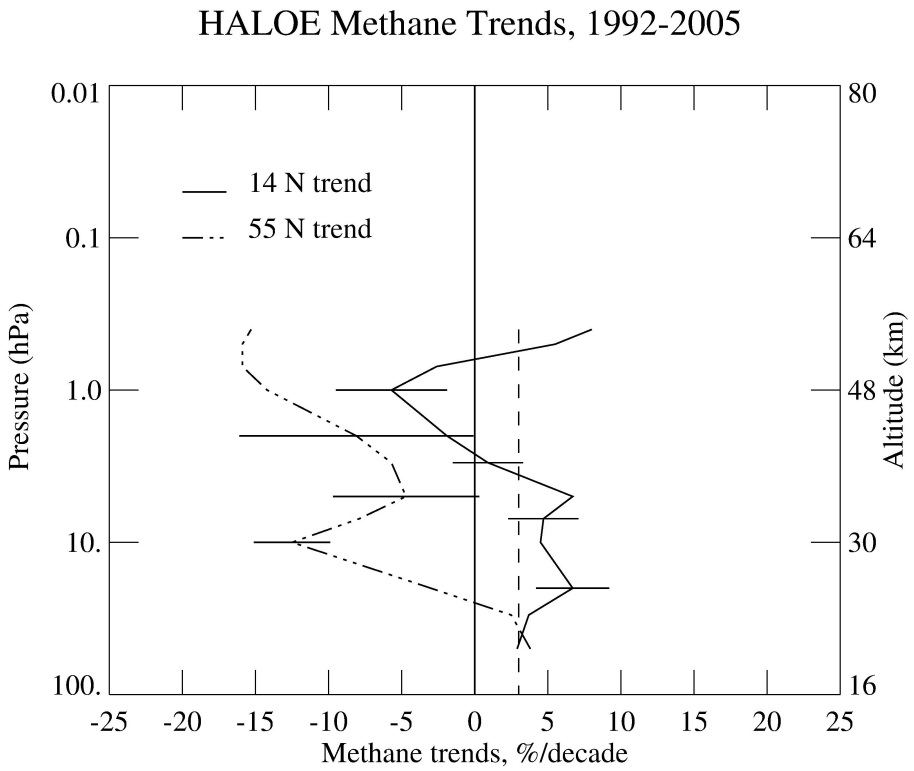

Figure 7. As in Fig. 6, but for the Northern Hemisphere.

ACPD
14, 24183–24220, 2014

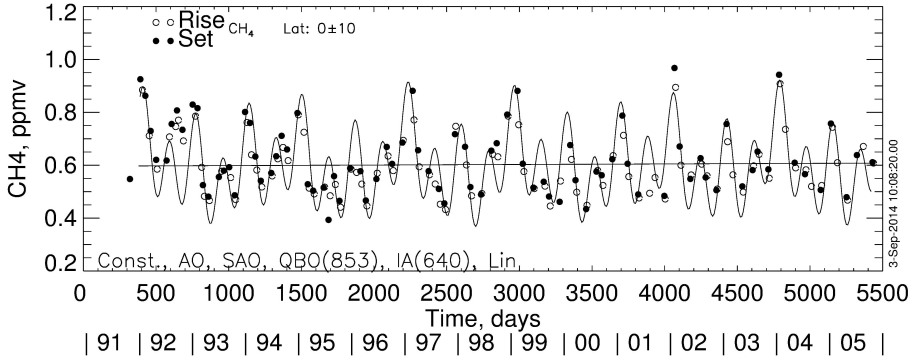

Figure 8. Time series of HALOE CH_4 at 2 hPa at low latitudes for comparison with that of Nedoluha et al. (1998).

ACPD
14, 24183–24220, 2014

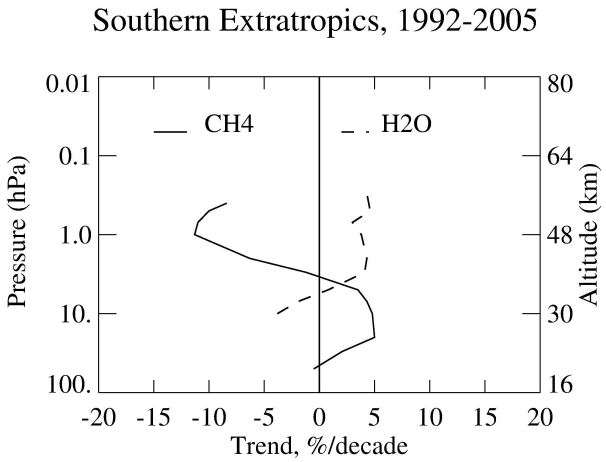

Figure 9. Extratropical trend profiles for CH_4 and H_2O for the Southern Hemisphere.

ACPD
14, 24183–24220, 2014

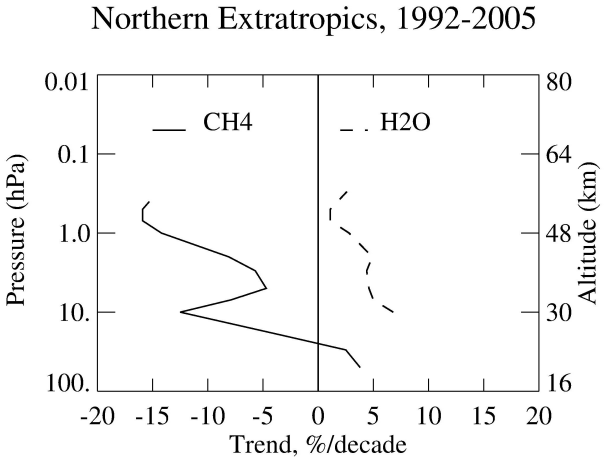

Figure 10. As in Fig. 9, but for the northern extratropics.

ACPD
14, 24183–24220, 2014

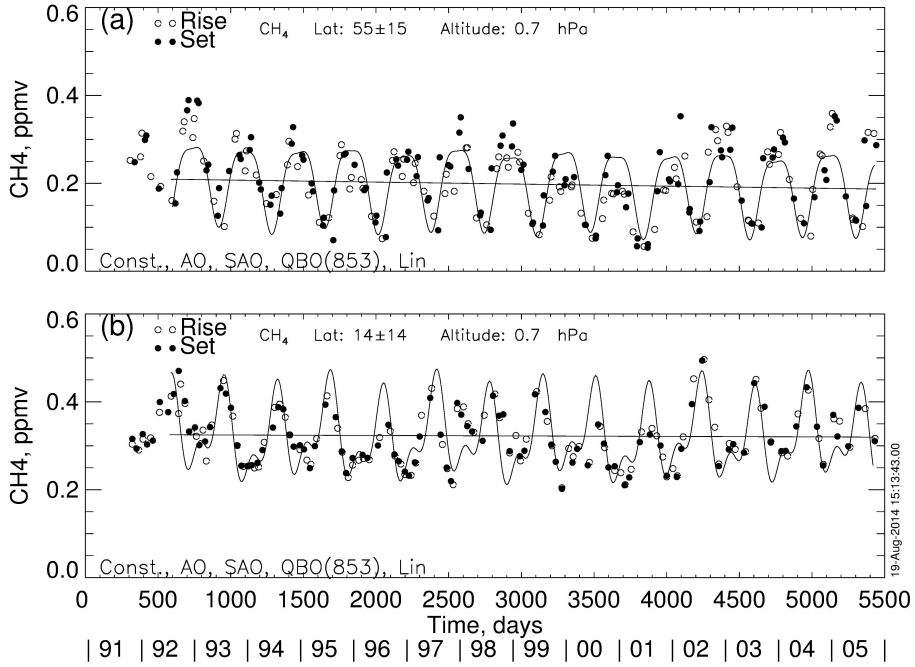

Figure 11. As in Fig. 3, but for CH_4 at 0.7 hPa in the northern **(a)** extratropics and **(b)** subtropics.

ACPD
14, 24183–24220, 2014

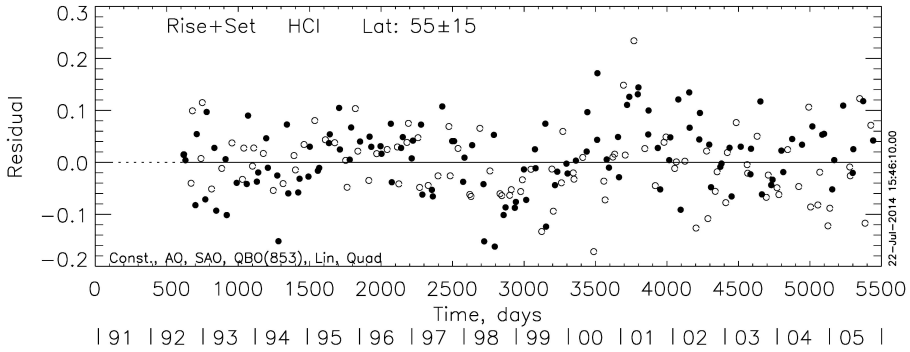

Figure 12. Time series of HCl residual (data – MLR curve) at 0.7 hPa and for the 55° N zone.

ACPD
14, 24183–24220, 2014

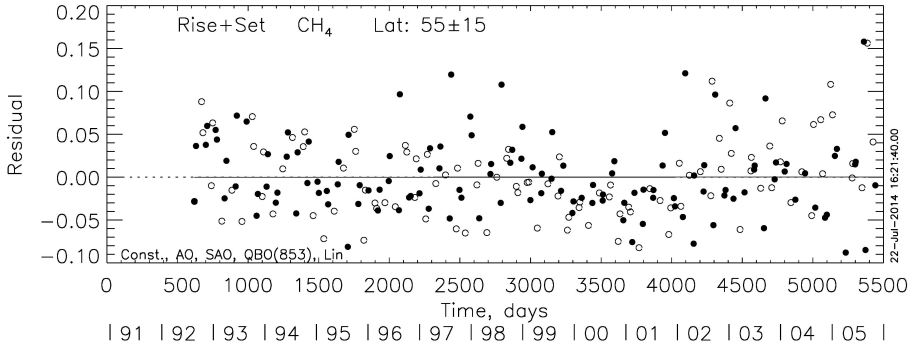

Figure 13. As in Fig. 12, but residual for CH_4.

ACPD
14, 24183–24220, 2014